Using Local Structure for the Reliable Removal of Noise from the Output of the LoG Edge Detector

Ahmad A. Masoud and Mohamed M. Bayoumi

Abstract—**This paper tackles an important problem in image processing; that is, the detection of edges in natural scenes. A scheme that combines simplicity with the ability to detect intensity jumps at widely varying contrasts is proposed. The scheme is constructed by combining the Laplacian-of-Gaussian (LoG) edge detector with a noise removal mechanism. The mechanism is built around a proposed definition for potentially valid edge contours that incorporates their local structure in the filtering process. Some of the advantages of the proposed approach include accurate localization of the edges and ease of implementation. Simulation results as well as statistical analysis of the approach for the 1-D case are provided.**

I. Introduction

EDGE detection has attracted the attention of researchers for over two decades. The prime motivation behind such an interest is due to several results [1], [2] conjecturing that the edges of an image and the structure of intensity surrounding them contain much of the essential information about the scene; therefore, offering a compact and, if performed properly, rich representation of the image. The problem is by no means simple, with difficulties starting as early as defining what an edge is [3]. Its importance is central to areas like machine vision, navigation, coding and restoration of images, as well as scene representation and understanding. Understandably, the literature tackling this problem is huge, and the principles employed for the solution are diverse [4]–[14]. In a recent article surveying the state of the art in edge detection [15], it was noted that "edge detection techniques are reaching a performance plateau in which increased sophistication is not producing a commensurate improvement in performance". It was also concluded that "further hammering of the problem at the signal level will prove largely fruitless". While we strongly agree with the first claim, we believe, as shown in this work, that improvements in terms of reducing complexity and enhancing performance can still be achieved by tackling the problem at the signal level.

This work is concerned with the development of an edge detection scheme that can extract edges from natural scenes, and have a reasonable level of complexity. What makes the task difficult is the wide range of contrasts an edge can assume in a natural scene. These contrasts may vary from the very visible to the hardly seen. Yet, they may all hold equal values as far as scene interpretation is concerned. Adding to this is the amount of computation that is required, especially when a high resolution sequence of images is to be processed. Here, a detection scheme is suggested that combines a small scale LoG operator with a noise filter that removes spurious responses from its output. The noise removal mechanism uses the local structure of the zero crossing (ZC) contours which mark the potential edges of the scene for filtering out noise. For the 1-D case the distance between successive ZC is used to judge the validity of the edges. Additional considerations that are mandated by the complex nature of natural scenes are introduced for the 2-D case. The proposed scheme is found capable of accurately localizing the edges. It is also easy to implement.

The paper is organized as follows. Section II reviews the LoG edge detection scheme and some methods for removing noise from its output. Section III discusses the proposed approach. In section IV, the performance of the proposed detector is statistically analyzed for the 1-D case. Section V contains simulation results. Conclusions are presented in section VI.

II. The Laplacian-of-Gaussian Detector

One of the popular techniques for edge detection utilizes the Laplacian-of-Gaussian operator (LoG) proposed by Marr and Hildreth [16]. In this technique, the edges are located as the zero crossings (ZC) of the convolved signal with the Laplacian of the Gaussian function which is given by

$$E(x) = \{x: \nabla^2 G(x,\sigma)^* I(x) = 0\}$$
$$G(x,\sigma) = \frac{1}{\sigma\sqrt{2\pi}} \exp(-x^2/2\pi\sigma^2) \quad (1)$$

where $E(x)$ is the set of detected edges, G is the Gaussian function, σ is the scale of this function, and $I(x)$ is the input signal to the LoG operator. Among the properties of this technique are efficient implementation [17], accurate localization [18], [19], orientation invariance, high sensitivity, and ability to produce closed edge contours [20]. Although high sensitivity is useful in detecting weak edges, it results in noise response that typically renders the output virtually unusable. One approach to alleviate this problem is to choose the scale (σ) large enough to smooth the signal. Unfortunately, increasing σ increases the computational load, reduces the resolution, increases the chance of having Phantom edges [21], and most importantly it causes a dislocation in the position of the estimated edges [22]. Edge dislocation prevents the measurement of valuable information about the intensity structure around the edge contours and distorts the shape

Manuscript received March 14, 1993; revised March 24, 1994.

The authors are with the Robotics Laboratory, Department of Electrical Engineering, Queen's University, Kingston, Ontario, Canada K7L-3N6.

IEEE Log Number 9405705.

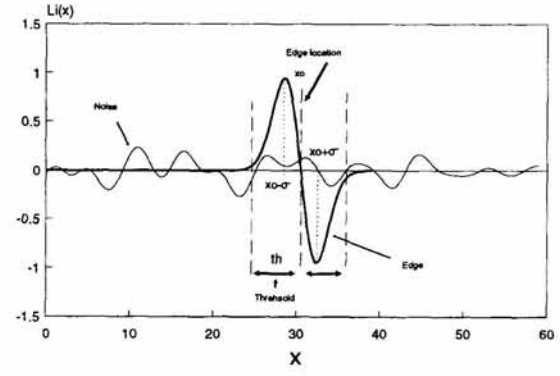

Fig. 1. Signal and Noise components from the LoG operator.

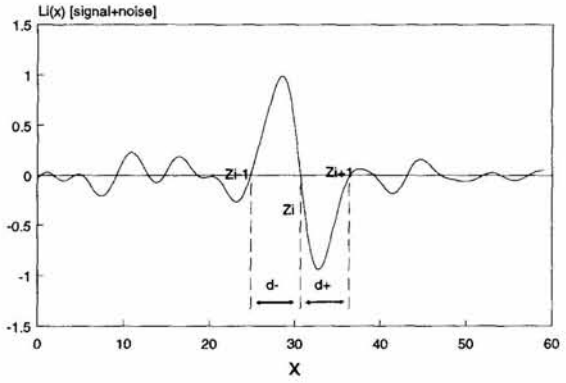

Fig. 3. Net signal from the LoG.

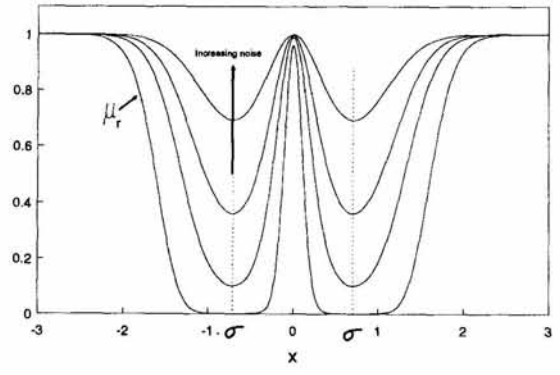

Fig. 2. Relative density of the zero crossings in the presence of an edge. σ is constant, σ_n is variable.

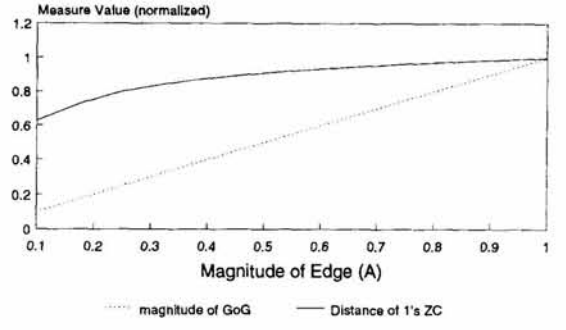

Fig. 4. $d+$ and |GoG| versus the edge contrast (A).

of objects. Other methods for counteracting the effect of noise can be found in [23], [24], [25], [31]. A simple and popular method to remove noise starts by employing a measure of the strength of the edge. To discriminate between false and valid edges, a threshold is then used. In [26] the slope of the convolved signal at the ZC (equivalent to the third derivative of the signal) was used as a measure of the edge strength. A more robust measure utilizes the magnitude of the signal convolved with the Gradient-of-Gaussian (GoG) [27], [28], [29]. A limitation of edge strength measures is the conflicting requirements between noise removal which requires a sufficiently high threshold, and retaining weak edges which requires a relatively low threshold. If a static threshold is chosen, only a compromise can be achieved. Moreover, all of the valid edges falling under the threshold are lost regardless of the noise intensity at that location. This prompted Canny [30] to use optimal filtering to locally estimate the noise and the signal in order to generate an adaptive threshold and reduce the loss of valid edges. Although an adaptive threshold improves the performance, it is computationally expensive. Furthermore, it encounters difficulties in detecting structures of minute jumps in intensity lying in natural scenes.

Our approach to identifying a false zero from a valid one begins with a search for a signature (i.e. a pattern that is with high probability associated with and only with the phenomenon of interest) in the output of the LoG operator that a sudden change in intensity leaves on the neighborhood of the corresponding ZC. For the signature to be usable as a basis of discrimination it has to be measurable such that a zero value of the measure is an indication that the ZC under consideration is definitely false; while a full value of the measure means that the ZC is valid (i.e. is generated by an underlying sudden jump in intensity). The level of confidence in the validity of the ZC monotonically increases with the value of the measure. To enable the construction of a low complexity discrimination mechanism, the chosen measure should be easily computable from the signature. It must also be weakly coupled to the signal energy. This enables it to exhibit an acceptable level of stationarity with respect to the widely varying contrast of the edges in a natural scene. This in turn reduces the need for adaptation by utilizing a noise removal mechanism, and it reduces the complexity of the edge detection scheme.

In this paper we show that the normal intervals between the successive zero crossings contours of the signal from the LoG operator provide the desired feature. Using only a simple static threshold, this approach is expected to provide a discrimination mechanism which can both reliably retain valid ZC's and effectively remove false ones. Since the burden of noise removal is transferred to the discrimination mechanism, the operator scale (σ) can be kept small for high resolution and accurate localization.

Fig. 5. ZC contours of an aerial image.

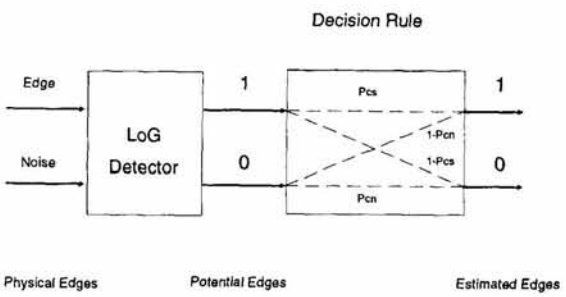

Fig. 6. Equivalent binary channel model of the decision rule.

III. The Proposed Approach

Our goal is to develop a procedure that can discriminate between a ZC generated by a valid edge $(I_1(x) = Au(x) + n(x))$, and a ZC generated by noise only $(I_2(x) = n(x))$. For convenience in the analysis, the edge is assumed to be an ideal step jump $(u(x))$ with a magnitude (A), such that

$$u(x) = \begin{cases} A & x \geq 0 \\ 0 & x < 0 \end{cases}.$$

The noise is assumed to be a stationary Additive White Gaussian Noise (AWGN) with zero mean and variance σ_n^2.

Let $L_i(x)$ and $D_i(x)$ be

$$L_i(x) = I_i(x)^* \nabla^2 G(x), \qquad D_i(x) = I_i(x)^* \nabla G(x).$$

For the 1-D case, an ideal edge yields

$$\nabla^2 G(x)^* u(x) = -\nabla G(x), \qquad \nabla G(x)^* u(x) = G(x). \quad (2)$$

where $*$ denotes convolution. Fig. 1 shows the signal and noise components of L_i. If an edge is present, L_i consists of the sum of both the GoG produced by the edge and scaled by A, and

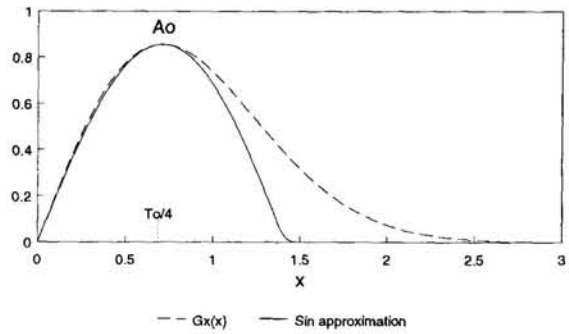

Fig. 7. Sinusoidal approximation of the $\nabla G(x)$. – – $G_x(x)$ —Sin approximation.

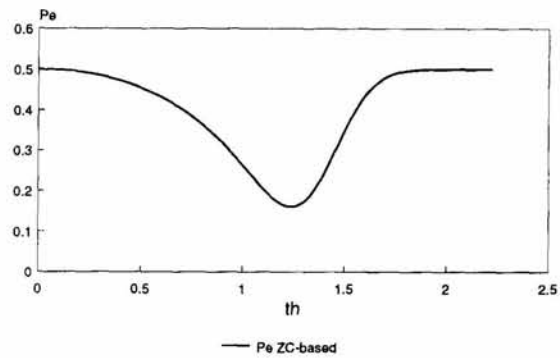

Fig. 8. P_e versus the for the ZC-based method.

the filtered noise. The ZC of the GoG marks the location of the edge (the edge may be displaced because of noise). Since the GoG has its highest slope at its ZC with the magnitude peaking around it, a local region depleted of ZC's is expected to exist on both sides of the ZC contours that mark true edges. This can also be concluded from the work of Tagare and deFigueiredo [18] where they derived the relative density of ZC's for $L_i(x)$ as a function of $x(\mu_r(x))$ as

$$\mu_r(x) = \exp\left[-\left(x \cdot \exp\left(-\frac{x^2}{\sigma^2} \right) \right)^2 \Big/ (2\sigma_n^2) \right]. \quad (3)$$

In Fig. 2 μ_r is drawn for different values of signal to noise ratio (SNR). From these observations it is expected that on the average the distance between successive ZC's of L_i when only noise exists is less than the distance between a valid ZC and the first false zero (this will be further discussed in the next section). Therefore, the validity of a ZC (Z_i) may be tested by computing $d_i- = \text{dist}(Z_i, Z_{i-1})$, and $d_i+ = \text{dist}(Z_{i+1}, Z_i)$. The following rule is then used to accept or reject Z_i (Fig. 3)

$$\begin{array}{ll} \text{if } [(d_i- \geq \text{th}) \text{ and } (d_i+ \geq \text{th}] & Z_i \text{ is Valid} \\ \text{else} & Z_i \text{ is False} \end{array} \quad (4)$$

where th is a selected threshold. Using the distance between successive zeros as a basis for discrimination has the advantage of weakening (compared to an energy-based discrimination measure) the coupling between the detector performance and the fluctuating contrasts of the edges. For a relatively wide

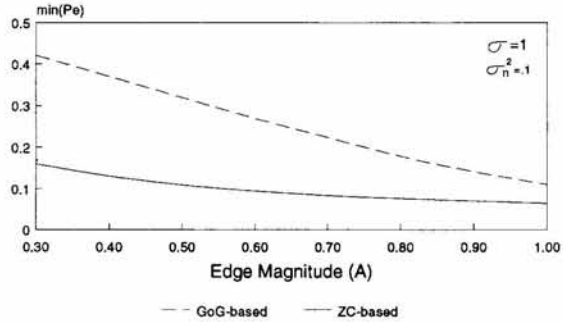

Fig. 9. Minimum achievable P_e for both the ZC-based and GoG-based methods.

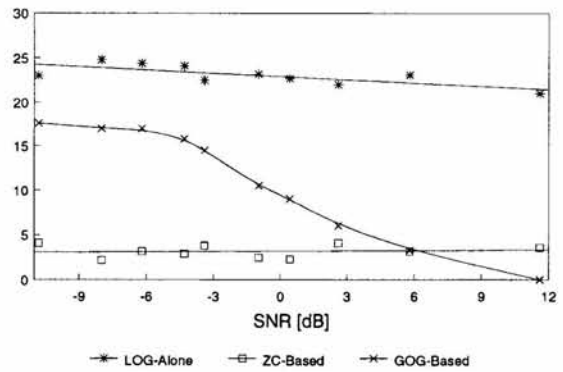

Fig. 10. Average number of false components.

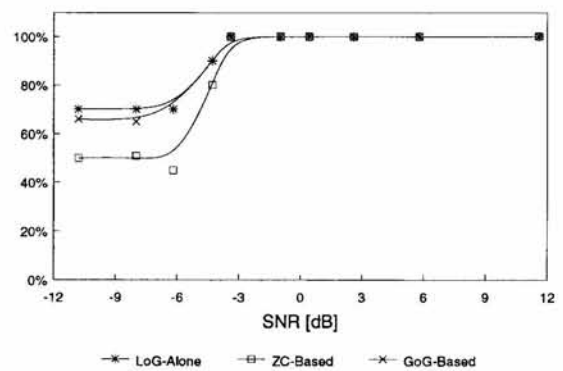

Fig. 11. Percentage correct detection.

range of SNR, it can be shown that the operator scale σ, which is constant, is the major deciding factor in determining $d+$ and $d-$. In Fig. 4 the magnitude of the output from both the GoG (D_i) and $d+$ are plotted for a small fixed noise power as a function of the contrast (A) when an edge is present. It can be seen that $d+$ is much less sensitive to changes in A than $D_i(x)$.

A. The 2-D Case

For the 2-D case d_i- and d_i+ are computed along both sides of the normal to the edge contours. The validity of this

Fig. 12. Original Test image.

approach is visually illustrated with an enlarged section of the zero contours of an airport aerial image that is processed by the LoG operator (Fig. 5). The presence of depletion regions in the vicinity of major edges is obvious.

The 2-D case is fundamentally different from the $1-D$ case. Here, the edges are no longer simple isolated points; instead they form zero contours that reflect, among other things, the complex geometry of the underlying scene. To define what is to be accepted as a valid edge contour and what is to be discarded as noise is, probably, more related to psychology than it is to engineering. Nevertheless, it is possible to come up with a useful technical definition of a valid edge that serves as a basis for filtering out noise. The selection procedure is based on the following:

1) Strongly visible edge contours ($|D_i| \geq \mathrm{th1}$) with a length that exceeds a certain value (in the experiments which we conducted, the contours are required to be more than two pixels in length) are considered to be valid edges.
2) Zero contours with very low contrasts ($|D_i| < \mathrm{th2}$, $\mathrm{th1} \gg \mathrm{th2}$) are considered too unreliable to be detected from a single frame image; therefore, they are rejected as noise.
3) Contours with strength that lies in between ($\mathrm{th1} > |D_i| \geq \mathrm{th2}$) are judged based on their saliency (e.g. if the length of a contour exceeds a certain threshold it is classified as valid; otherwise, it is rejected as noise. Same consideration is given to the depletion region; however, a region with single pixels in width is found to be satisfactory in the tested cases). Contours that are generated from an underlying object and fall in this category are called weak edges.

It ought to be mentioned that an edge contour consists of a series of connected pixels (single pixel wide) that are surrounded by zero depletion regions from both sides. It is to be noted that as a basis of discrimination the local structure of

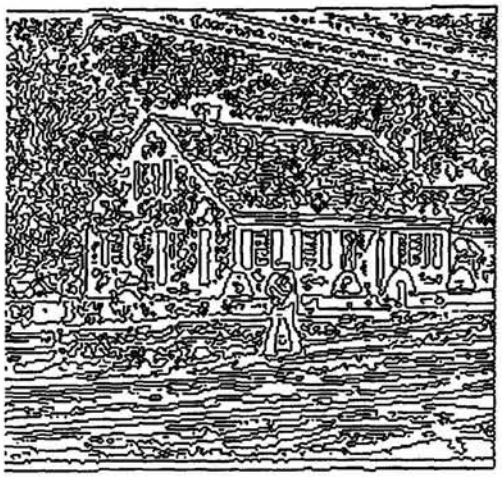

Fig. 13. Edge contours from the LoG only.

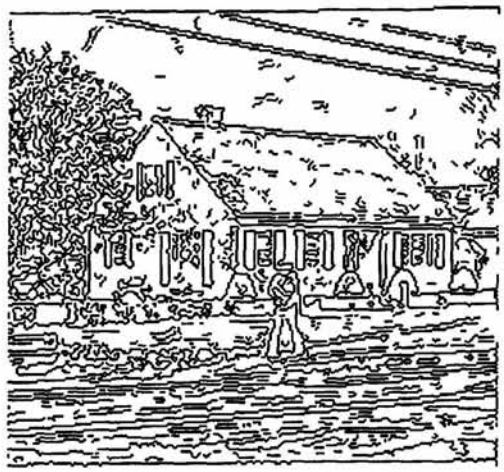

Fig. 15. Same as Fig. 14, but th = 3 samples.

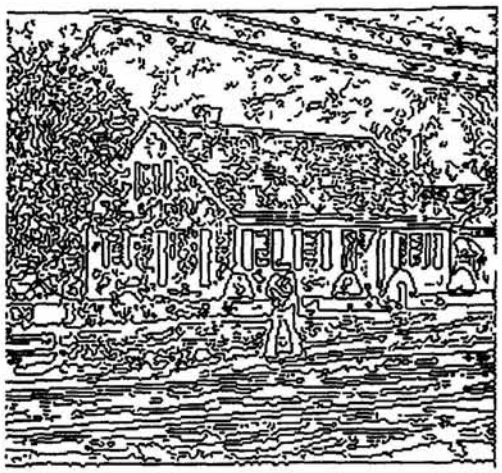

Fig. 14. Noise removal using proposed method, procedure 1, th = 4 samples.

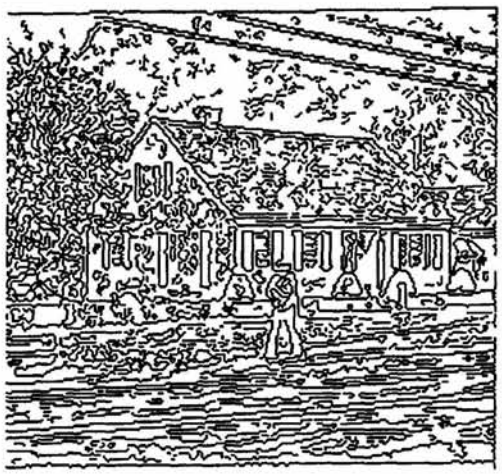

Fig. 16. Noise removal using proposed method, procedure 2, th = 3 samples.

the ZC contours that correspond to valid edges is less variant than the associated contrasts, and is highly Likely to reflect the stationary geometry of the underlying objects in the scene. It is unlikely that the structure of the ZC contours will vary with the color of the object, its background, or the Lighting conditions. All these factors considerably affect the contrast of the contours which makes the compensation for their presence in the edge detection process quite a cumbersome task, if at all possible. On the other hand, local structure provides a reasonable level of stationarity which proves very useful for constructing a relatively reliable, low complexity detector. As for the noise (white, or at least wide-band boise is considered), since the scale of the LoG is kept small the resulting ZC contours are most probably random unstructured noise webs, which are highly unlikely to produce salient components.

Using the local structure to filter valid edges requires no additional multiplications, and has both performance and implementation advantages over a purely energy-based approach to edge detection [27].

B. Structure-Based Filtering Mechanisms

After the signature that distinguishes a valid edge from a false one is identified, it remains to construct a procedure (a mechanism) for utilizing such a signature for filtering out (what is perceived to be) noise. In the following, two procedures are suggested for utilizing the ZC depletion regions that surround valid edge contours.

Procedure 1: Assume that Z_{ij} is the ZC that is being examined. since valid ZC contours are most probably one pixel in width, and are surrounded by ZC depletion regions, while contours that are generated by noise are randomly scattered webs, Z_{ij} can be judged by counting the number of ZC's inside a local window that is centered around the examined ZC. If the number of ZC's exceeds a certain threshold (for the time being the threshold is experimentally determined), the zero crossing is discarded as noise; otherwise, it is accepted as valid. It is to be noticed that for such a procedure to work the scale of the LoG (σ) has to be small. As for the width of

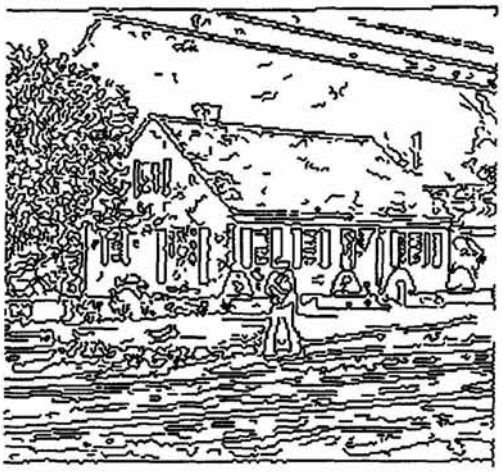

Fig. 17. Same as Fig. 16, but th = 11 samples.

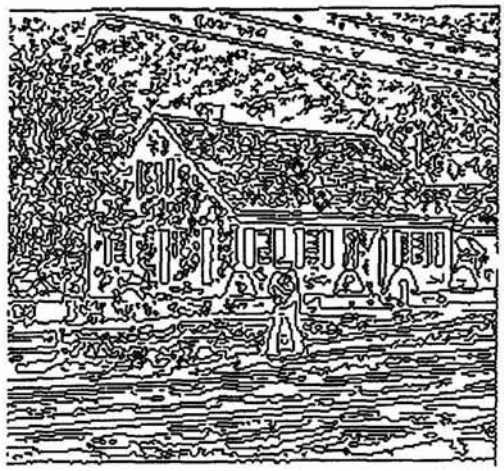

Fig. 18. Noise removal using GoG, th = 0.2%.

the window, it is dependent on the size of the depletion region which in turn is dependent on the scale of the LoG. However, for all the cases that we tested the performance of a 3×3 window was always satisfactory.

Procedure 2: Here, the validity of Z_{ij} is judged based on the length of the contour to which it belongs. The width of the depletion region could also be used. However, we observed that using a fixed one pixel depletion width in conjunction with the length of the contour produces a satisfactory filtering effect. If the length of the contour exceeds a certain value the Z_{ij} is accepted as valid; otherwise, it is discarded as noise.

The first procedure is characterized by its simplicity and ease of extension to the M-D case (e.g., for a 3-D image sequence the number of ZC's can be counted in a $3 \times 3 \times 3$ cube). On the other hand, the second procedure allows more control and enhances the selectivity of the filtering process.

IV. Analysis (1-D)

Since the function of the decision rule is to transmit or block a Zero from the LoG operator, it is substituted by a binary channel equivalence to facilitate the analysis (Fig. 6). A "one" at the channel input indicates a ZC from the LoG that marks a correct edge; while a "zero" indicates a ZC that is caused by noise. A "one" at the output indicates that a potential edge is accepted, while a "zero" indicates that a potential edge is rejected. The performance of the detector is analyzed by combining the misdetection probability $(1 - P_{\rm cs})$, with the false detection probability $(1 - P_{\rm cn})$ to compute the probability of error (P_e)

$$P_e = P_1(1 - P_{\rm cs}) + P_0(1 - P_{\rm cn}) \tag{5}$$

where $P_{\rm cs}$ is the probability that a valid ZC is decided as an edge, $P_{\rm cn}$ is the probability that a false ZC is discarded. P_1 is the probability that a valid ZC occurs at the output of the LoG operator, and P_0 is the probability that a false ZC occurs. There are several factors on which P_1 and P_0 depend. Some of these are the signal richness in edges, the characteristics of noise, and the scale of the LoG operator

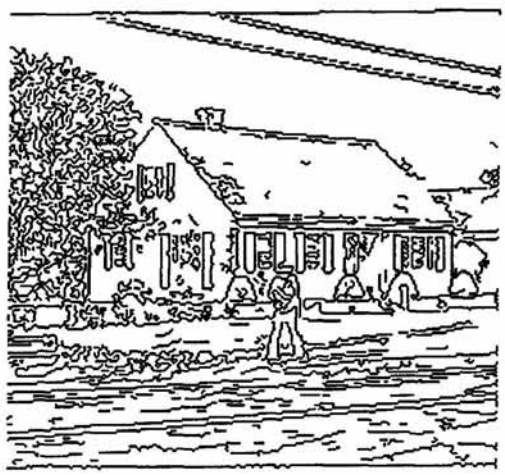

Fig. 19. Noise removal using GoG, th = 5.0%.

(σ). However, since P_1 and P_0 are not known a priori, they are assumed to be equal $(P_1 = P_0 = 0.5)$ for convenience in the analysis. The performance of the GoG-based rule (energy-based) is compared with that of a ZC-based rule using their probability of error.

A. The ZC-Based Method

To compute the performance probabilities of this scheme, one needs to compute the following autocorrelations and Conditional Probability Distribution Functions (PDF's). The autocorrelation of the noise at the LoG input $(R_i(\tau))$ and output $(R_o(\tau))$ are

$$R_i(\tau) = \sigma_n^2 \delta(\tau) \tag{6}$$
$$R_o(\tau) = \frac{\sigma_n^2}{\sigma^7}\sqrt{\frac{\pi}{2}}[3\sigma^4 - 6\sigma^2\tau^2 + \tau^4]e^{-\tau^2/2\sigma^2}$$

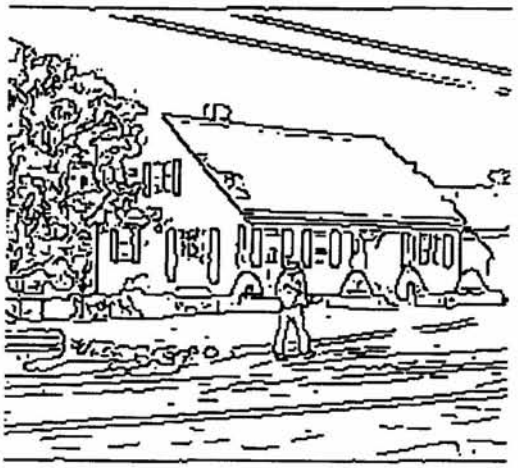

Fig. 20. Edges from Canny detector.

Fig. 21. Edges using an Energy-based method.

where $\delta(\tau)$ is the Kronecker delta function. The variances of the noise at the input and output (σ_i^2, σ_0^2) are

$$\sigma_i^2 = \sigma_n^2, \qquad \sigma_o^2 = 3\sqrt{\frac{\pi}{2}}\left[\frac{\sigma_n^2}{\sigma^3}\right]. \tag{7}$$

The conditional PDF's are: $P_{\rm no}(\tau)$ which is the conditional probability that the first ZC after time t occurs between $t+\tau$ and $t+\tau+d\tau$ given a ZC at time t when the input to the LoG is I_2 (noise only). The second conditional PDF is $P_{\rm so}(\tau)$ which is defined similar to $P_{\rm no}(\tau)$ except that it is computed when the input to the LoG is I_1 (noise + edge). For a smooth zero mean Gaussian noise, McFadden [32], [33] derived an approximation to $P_{\rm no}$ as

$$P_{\rm no}(\tau) \simeq \frac{\rho''(\tau)(1-\rho(\tau)^2) + \rho(\tau)\rho'(\tau)^2}{2\sqrt{\rho''(0)}[1-\rho(\tau)^2]^{3/2}} \tag{8}$$

where $\rho(\tau)$ is the normalized auto correlation function, ρ' and ρ'' are the first and second derivatives of ρ with respect to τ. Better approximations that may be used to derive $P_{\rm no}$ were provided by Longuet-Higgins in [34]. However, McFadden's approximation is the one adopted here because of its simplicity and reasonable accuracy. Assuming that the intervals between successive ZC's of the output noise are independent, the probability of validating a false ZC is given by

$$\left[1 - \int_0^{\rm th} P_{\rm no}(\tau)d\tau\right]^2. \tag{9}$$

To compute $P_{\rm so}(\tau)$ we shall first approximate the GoG as

$$G_x(x) = \frac{2A}{\sigma^2}xe^{-\frac{x^2}{\sigma^2}} \simeq \begin{bmatrix} A_0 \sin\left(\dfrac{2\pi}{T_0}x\right) & |x| \le T_0/2 \\ 0 & |x| \ge T_0/2 \end{bmatrix} \tag{10}$$

where $T_0 = 4x_m$, $x_m = \sigma/\sqrt{2}$, $A_0 = \sqrt{2}\cdot e^{-1/2}A/\sigma$, x_m is the distance at which G_x reaches its peak, and A_0 is the corresponding magnitude. Fig. 7 shows the GoG and its approximation. It can be seen that the fit is good for $|x| \le x_m$. However, for $|x| > x_m$ the approximation has a lower magnitude which is acceptable since it will provide a lower bound on $P_{\rm so}$. Using this approximation one can use the result by Cobb [35] for the distribution of intervals between the ZC's of a sinwave in AWGN, which is

$$P_{\rm so} \simeq \frac{\pi^{1/2}(A_0/\sigma_n^2)}{2\cdot(1+\rho(1))^{1/2}} \cdot \exp\left(-\frac{\pi^2(A_0/\sigma_n^2)^2}{4\cdot(1+\rho(1))}\cdot(\tau-1)^2\right). \tag{11}$$

This distribution is accurate for moderate values of SNR. For moderate values of SNR we shall assume that $d+$ and $d-$ are strongly dependent. Therefore, one gets [36]

$$\begin{aligned} P(d+ > {\rm th}, d- > {\rm th}) &= P(d+ > {\rm th}/d- > {\rm th})P(d- > {\rm th}) \\ &\simeq 1 \cdot P(d- > {\rm th}) = P(d+ > {\rm th}) \end{aligned}$$

and $P_{\rm cs}$ can be computed as

$$P_{\rm cs} \simeq 1 - \int_0^{\rm th} P_{\rm so}(\tau)d\tau \tag{12}$$

Fig. 8 shows the P_e of this scheme as a function of the threshold th for a fixed value of σ_n^2.

B. The GoG-Based Scheme

Here, $P_{\rm cs}$ and $P_{\rm cn}$ are computed for the following decision rule

$$\text{if} \quad \begin{matrix} |D_i(x)| \ge {\rm th} & Z_i \text{ is valid} \\ |D_i(x)| < {\rm th} & Z_i \text{ is false} \end{matrix} \tag{13}$$

To do this one needs to compute the following conditional PDF's: $P_{\rm so}(a) = P(a < D_i(x) \le a + da | L_i(x) = 0)$ when the input is I_1, $P_{\rm no}$ is defined similarly, but the input is then given by I_2. The autocorrelation of the noise at the output of the GoG and its variance are given by

$$\begin{aligned} R_o(\tau) &= \frac{\sigma_n^2}{\sigma^3}\sqrt{\frac{\pi}{2}}[\sigma^2 - \tau^2]e^{-\tau^2/2\sigma_n^2} \\ \sigma_o^2 &= \frac{\sigma_n^2}{\sigma}\sqrt{\frac{\pi}{2}}. \end{aligned} \tag{14}$$

Since the noise is Gaussian and the GoG is a linear operator, the output noise is also Gaussian. Assuming a relatively high

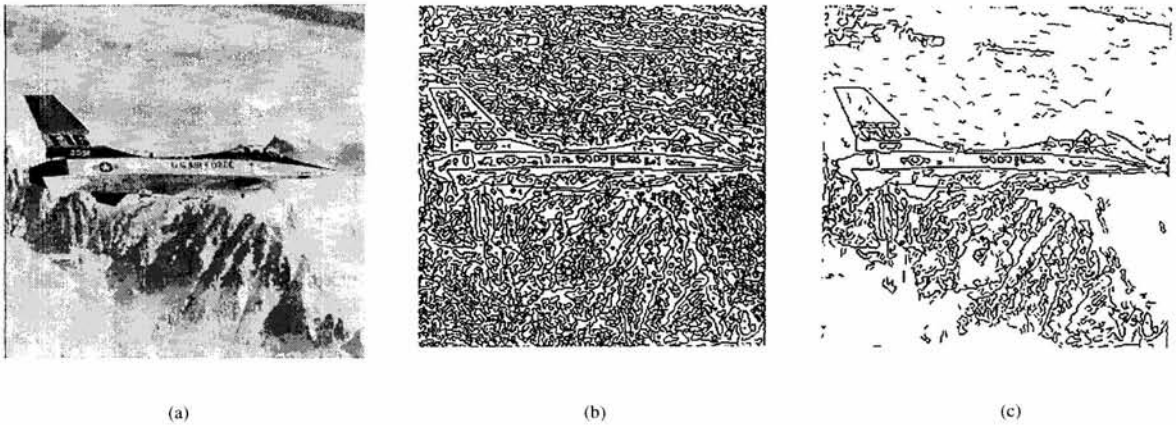

(a) (b) (c)

Fig. 22. (a) F16; (b) F16, output of LoG; (c) F16, output of the filter.

(a) (b) (c)

Fig. 23. (a) Lenna; (b) Lenna, output of LoG; (c) Lenna, output of the filter.

SNR an a small σ, the dislocation in the position of the edge can be disregarded and P_{so}, as well as P_{no} are approximated as

$$P_{\text{so}}(a) \simeq \frac{1}{\sigma_o\sqrt{(2\pi)}} e^{-(a-A)^2/(2\sigma_o^2)}$$
$$P_{\text{no}}(a) \simeq \frac{1}{\sigma_o\sqrt{(2\pi)}} e^{-a^2/(2\sigma_o^2)} \quad (15)$$

whereas P_{cn}, P_{cs} can be computed as

$$P_{\text{cn}} = \int_{-\text{th}}^{\text{th}} P_{\text{no}}(a)da, \qquad P_{\text{cs}} = 1 - \int_{-\text{th}}^{\text{th}} P_{\text{so}}(a)da. \quad (16)$$

Fig. 9 shows the minimum achievable P_e versus A for a fixed value of σ and σ_n^2. This was obtained using the optimum threshold. It should be pointed out that since P_{cn} for the ZC-based rule depends only on the normalized auto-correlation function ($\rho(\tau)$) where no information about the power of the noise or the strength of the edge (A) is present, the number of falsely detected components does not depend on the SNR (A Constant False Alarm Detector). This is in contrast to the GoG-based detector where the number of detected false components increases as the SNR decreases. This is demonstrated by an example in the next section.

V. Results

The proposed scheme is tested using the following 1-d discrete signal

$$S(n) = u(n-25) + N(n).$$

The size of the LoG operator is 13 samples with scale $\sigma = 1$, and the size of the data record is 90 samples. At least two samples before and after a ZC have to be free of zero crossings for the ZC to be considered valid. The GoG-based scheme was also simulated with a threshold of 10% from its output maxima. The experiment is repeated several times at different signal to noise ratios. Figs. 10 and 11 show respectively the average number of detected false components, and the percentage detection of the correct component for the LoG alone, the GoG-based, and the ZC-based schemes. As can be seen the number of false components from the ZC-based filter is significantly less than that from the LoG operator with values closely fluctuating around a constant as the SNR varies.

While the number of false components from the GoG-based filter is lower for high SNR, it significantly increases as the SNR decreases till it finally settles at a much higher value than that of the ZC-based filter. As for the percentage of times the correct component was detected, the performance of the two methods remain close for a wide range of SNR with the GoG-based method having a higher percentage of detection than the ZC method at very low SNR.

The detector is also tested for the 2-D case. The test image in Fig. 12 is chosen to include rough and smooth regions, and edges of widely varying contrasts. The image size if 256×256, and the size of the operator is 7×7 with a scale $\sigma = 1$. Fig. 13 shows the edge contours from the LoG operator alone which, as can be seen, is highly contaminated with noise. In Figs. 14 and 15 the noise is filtered out using the proposed method. Contours having $|\mathrm{GoG}| \leq .002 \cdot \max|D_{ij}|$ are unconditionally rejected, those with $|\mathrm{GoG}| > .05 \cdot \max|D_{ij}|$ are unconditionally accepted, while those with $.002 \cdot \max|D_{ij}| < |\mathrm{GoG}| \leq .05 \cdot \max|D_{ij}|$ are judged based on the number of ZC's in a 3×3 window with a ZC declared as an edge if the count of zeros is less than or equal to 4, and 3 respectively. In Figs. 16 and 17 the second procedure that is given in section III is used to judge edge contours with $.002 \cdot \max|D_{ij}| < |\mathrm{GoG}| \leq .05 \cdot \max|D_{ij}|$. Here, the width of the depletion region is fixed to at least one pixel. For the ZC to be accepted as valid the length of the contour to which it belongs has to be greater than or equal to 3, and 11 pixels respectively. For both procedures single and double isolated pixels are removed from the final output. In Figs. 18, 19 only the magnitude of the GoG is used to filter the noise with thresholds set to $.002 \cdot \max|D_{ij}|$ and $.05 \cdot \max|D_{ij}|$ respectively. As can be seen the first threshold is too small to achieve significant reduction in noise, while the second threshold, although small (5% only) causes a significant loss in low intensity edges (compared to the edges that were detected with the proposed method). Fig. 20 shows the edges from the well-known Canny detector. The loss of the edge structure in the detail of the image is illustrated using this large scale operator. Fig. 21 shows the output of an approach that intensively utilizes an energy functional for edge detection [37]. Figs. 22(a) and 23(a) show two natural scenes that are to be processed using the proposed method. Figs. 22(b) and 23(b) show the output from the LoG operator that is used to process the above images. The following procedure is used to filter out noisy ZC contours: contours having $|\mathrm{GoG}| \leq 0.025 \cdot \max|D_{ij}|$ are unconditionally rejected, those with $|\mathrm{GoG}| > .07 \cdot \max|D_{ij}|$ are unconditionally accepted, while those with $.025 \cdot \max|D_{ij}| < |\mathrm{GoG}| \leq .07 \cdot \max|D_{ij}|$ are judged based on the number of ZC's in a 3×3 window, where a ZC is declared as an edge if the count of zeros is less than or equal to 3; otherwise, it is rejected as noise. Figs. 22(c), 23(c) show the final output from the filtering mechanism.

VI. Conclusion

In this paper, two critical issues regarding edge detection are tackled. These are the reliability needed when acting on natural scenes, and an acceptable complexity level that makes the use of the detector feasible in computationally demanding situations. The demonstrated detector in this paper consists of the LoG edge detector combined with a noise removal mechanism. This approach leaves the scale of the LoG operator relatively free to be adjusted for high resolution, accurate localization, and high sensitivity. We believe that the simplicity and efficiency of the noise removal mechanism is the result of incorporating the local structure of the ZC contours (potential edges) in the discrimination process. This method proves to be less sensitive to fluctuations in the edge contrast and it requires less computation than an energy-based noise removal technique. The technique is proposed as a solution to the edge detection problem in situations where a small scale zero crossing detector must be used for accurate edge location, since it provides a method for reducing spurious responses inherent in such an operator.

References

[1] H. Barrow and J. Tenebaum, "Recovery of intrinsic scene characteristics from images," *Computer Vision Systems*, A. Hansa, E. Riseman, Eds. Academic Press, 1978.

[2] V. Kovalevsky, "Structural image analysis," *8th Int. Conf. Pat. Recog.*, Paris, pp. 27–31, 1986.

[3] J. Malik and P. Perona, "Finding boundaries in images," *Neural Networks for Perception Vol. 1: Human and Machine Perception*, Harry Wechsler, Ed. Academic Press, 1992, pp. 315–344.

[4] H. Tan, S. Gelfand, and E. Delp, "A comparative cost function approach to edge detection," *IEEE Trans. Syst. Man Cyber.*, vol. 19, no. 6, pp. 1337–49, Nov./Dec. 1989.

[5] G. Dattatreya and L. Kanal, "Detection and smoothing of edge contours in images by one-dimensional Kalman techniques," *IEEE Trans. Syst. Man Cyber.*, vol. 20, no. 1, pp. 159–165, Jan./Feb. 1990.

[6] O. Zuniga and R. Haralic, "Integrated directional derivative gradient operator," *IEEE Trans. Syst. Man Cyber.*, vol. 17, no. 3, pp. 508–517, May/Jun. 1987.

[7] J. Lee and Y. Fang, "A new method for edge detection and localization (Greens theorem)," *SPIE, Applicat. Artificial Intelligence VIII*, M. Trivedi, Ed., 17–19, April, Florida, 1990, pp. 524–535.

[8] H. Kawakami, "Selective edge detection based on harmonic oscillator wave functions," *SPIE, Applicat. Artificial Intelligence IX*, M. Trivedi, Ed., 2–4, April, Florida, 1991, pp. 156–166.

[9] P. Perona and J. Malik, "Boundary detection using quadratic filters: performance criteria and experimental assessment," *SPIE, Applicat.Artificial Intelligence X*, M. Trivedi, Ed., 22–24, April, Florida, 1992, pp. 326–340.

[10] R. Boie, I. Cox and P. Rehak, "Optimum edge recognition using matched filters," *IEEE Comp. Soc. Conf. Comp. Vision Pat. Recog.*, Miami, FL, June 22–26, 1986, pp. 100–108.

[11] A. Marteli, "An application of heuristic search methods to edge and contour detection," *Communication ACM*, vol. 19, no. 2, pp. 73–83, Feb. 1976.

[12] F. Catté, P. Lions, J. Morel, and T. Coll, "Image selective smoothing and edge detection by nonlinear diffusion," *SIAM J. Numer. Anal.*, vol. 29, no. 1, pp. 182–193, Feb. 1992.

[13] O. Morris, M. Lee, and A. Constantinides, "A unified method for segmentation and edge detection using graph theory," *ICASSP-86*, Tokyo, Japan, Apr. 7–11, pp. 2051–2054, 1986.

[14] A. Shiozaki, "Edge extraction using entropy operator," *Computer Vision, Graphics, and Image Processing*, vol. 36, pp. 1–9, 1986..

[15] K. Boyer and S. Sarkar, "Assessing the state of art in edge detection," *1992 SPIE: Mach. Vis. and Robotics*, Florida, 20–24, pp. 353–62, Apr. 1992.

[16] D. Marr and H. Hildreth, "Theory of edge detection," *Proc. Roy Soc. London*, B207, 1980, pp. 187–217.

[17] G. Sotak and K. Boyer, "The Laplacian-of-Gaussian kernel: A formal analysis and design procedure for fast, accurate convolution and full frame output," *Comp. Vis. Graph. and Image Proc.*, vol. 10, no. 5, Sept. 1988, pp. 147–189.

[18] H. Tagare and R. DeFigueiredo, "On the localization performance measure and optimal edge detection," *SPIE: Image Processing Algorithms and Techniques*, 12–14, Feb. 1990, California, pp. 408–16.

[19] S. Sarkar and K. Boyer, "On optimal infinite impulse response edge detection filters," *IEEE Trans. Pattern Anal. Machine Intell.*, vol. PAMI-13, Nov. 1991.
[20] A. Yuille and T. Poggio, "Scaling theorems for zero crossings," *IEEE Trans. Pat. Anal. and Machi Intel.*, vol. PAMI-10, no. 1, pp. 15–25, Jan. 1988.
[21] J. Clark, "Singularity Theory and Phantom Edges in Scale Space," *IEEE Trans. on Pattern Anal. Machine Intell.*, vol. PAMI-10, no. 5, pp. 720–727, Sept. 1988.
[22] Y. Leclerc and S. Zucker, "The local structure of image discontinuities in one dimension," *IEEE Trans. Pattern Anal. Machine Intell.*, vol. PAMI-9, no. 3, pp. 341–355, May 1987.
[23] Y. Lu and R. Jain, "Reasoning about edges in scale space," *IEEE Trans. Pattern Anal. Machine Intell.*, vol. PAMI-14, no. 4, pp. 450–467, Apr. 1992.
[24] S. Raman, S. Sarkar, and K. Boyer, "Tissue boundary refinement in magnetic resonance images using contour-based scale space matching," *IEEE Trans. Med. Imag.*, vol. 10, no. 2, pp. 109–21, Jun. 1991.
[25] S. Mallat and W. Hwang, "Singularity detection and processing with wavelets," *IEEE Trans. Inform. Theory*, vol. 38, no. 2, pp. 617–643, Mar. 1992.
[26] A. Asefi, "Implementation and evaluation of different edge detection techniques," *M.Sc. Thesis*, Electronics Engineering and Computer Science, University of California Davis, 1990.
[27] P. Kube, "Properties of energy edge detectors," *92 IEEE Comp. Soci. Conf. Comp. Vision. and Pat. Recog.*, June 15–18, IL, 92, pp. 586–591.
[28] O. Zuniga and R. Haralick, "Gradient threshold selection for edge detection," *Pat. Recog.*, vol. 21, no. 5, pp. 493–503, 1988.
[29] J. Haddon, "Generalized threshold selection for edge detection," *Pat. Recog.*, vol. 21, no. 3, pp. 195–203, 1988.
[30] J. Canny, "A computational approach to edge detection," *IEEE Trans. Pattern Anal Machine Intell.*, vol. 8, no. 6, pp. 679–698, 1986.
[31] H. Heong and C. Kim, "Adaptive determination of filters scales for edge detection," *IEEE Trans. Pattern Anal. Machine Intell.*, vol. PAMI-14, no. 5, pp. 579–585, May 1992.
[32] J. McFadden, "The axis-crossing intervals of random functions," *IRE Trans. Inform. Theory*, pp. 146–150, Dec. 1956.
[33] ——, "The axis-crossing intervals of random functions-II," *IRE Trans. Inform. Theory*, pp. 14–24, Mar. 1958.
[34] M. Longuet-Higgins, "The distribution of intervals between zeros of a stationary random function," *Phil. Trans. Roy. Soc., London*, vol. A254, pp. 557–599, 1962.
[35] S. Cobb, "The distribution of intervals between zero crossings of sin wave plus random noise and allied topics," *IEEE Trans. Inform. Theory*, pp. 220–233, Apr. 1965.
[36] A. Papoulis, *Probability, Random Variables, and Stochastic Processes*, 2nd Ed. McGraw-Hill, 1984.
[37] D. Geiger and A. Yuille, "A common framework to image segmentation," *Int. Jour. Comput. Vision*, vol. 6, no. 3, pp. 227–243, 1991.

Ahmad A. Masoud was born in Saudi Arabia in 1963. He obtained a B.Sc. degree in electrical engineering from Yarmouk University, Irbid, Jordan, in 1984, and M.Sc. in electrical engineering from Queen's University, Kingston, Ontario, Canada in 1989 and is currently completing a Ph.D. in electrical engineering from Queen's University. He worked as a research assistant at the Electrical Engineering Department at Jordan University of Science and Technology from 1984–1987. His currrent interests are edge detection, scene interpretation, path planning, and constrained motion control of robotics manipulators.

Mohamed M. Bayoumi received a B.Sc. degree in electrical engineering from the University of Alexandria, Egypt. He also received the "Diplom Mathmatiker" degree in applied mathematics from the Swiss Federal Institute of Technology, Zurich. From the same university, he received the Ph.D. degree in electrical engineering in 1963. He worked in the Research and Development Laboratory for Control System Design, in Landis and Gyr, Zug, Switzerland, from 1963–1969.

In 1969, Dr. Bayoumi joined the faculty at Queen's University, Kingston, Ontario, Canada, and he is currently a Professor of Electrical and Computer Engineering. His research interests lie in control systems, inlcuding adaptive control, in robotics and signal processing.